Nanomaterials and Nanotechnology

OPEN ACCESS
ARTICLE

Photoluminescence Quenching and Structure of Nanocomposite Based on Graphene Oxide Layers Decorated with Nanostructured Porphyrin

Omar Bajjou[1*], Precious Nametso Mongwaketsi[2,3], Mohammed Khenfouch [1,2,3], Anass Bakour [1,4], Mimouna Baïtoul[1*], Malik Maaza[2,3] and Jany Wery Venturini[4]

1 University Sidi Mohamed Ben Abdellah, Faculty of Sciences Dhar el Mahraz, Laboratory of Solid-state Physics, Group of Polymers and Nanomaterials, Atlas Fez, Morocco
2 UNISA Africa Chair in Nanosciences-Nanotechnology, College of Graduate Studies, University of South Africa, Muckleneuk Ridge, Pretoria, South Africa
3 iThemba LABS-National Research Foundation of South Africa, Old Faure Road, Western Cape Province, South Africa
4 Institut des Matériaux Jean Rouxel, Nantes, 2 rue de la Houssinière, Nantes, France
* Corresponding author(s) E-mail: baitoul@yahoo.fr, bajjou.omar@gmail.com

Received 04 November 2014; Accepted 19 January 2015

DOI: 10.5772/60111

Abstract

Nanocomposites based on few-layers graphene oxide (FGO) decorated with porphyrin nanorods (PN) were synthesized and the interfacial interaction between these two components was investigated by using scanning electron microscopy (SEM), photoluminescence spectroscopy, resonant Raman scattering and Fourier transform infrared (FT-IR) techniques. SEM showed good exfoliation of FGO and its successful interaction with the PN. The photoluminescence results showed an important interaction between FGO and PN resulting in a quenching of the photoluminescence of the PN-FGO composite. Resonant Raman with PN aggregates and FT-IR results revealed a π-π intermolecular interaction confirming the energy/charge transfer. Moreover, the investigation of X-ray diffraction confirmed the intercalation of PN in FGO and their disaggregation. The findings presented here are an important contribution to achieving the functionalization of graphene derivative surfaces with PN for various optoelectronic applications and particularly photovoltaic cells.

Keywords Graphene oxide, self-assembled porphyrin, photoluminescence, resonant Raman scattering, FT-IR, X-ray diffraction

1. Introduction

Over the past years, huge scientific interest has been focused on graphene due to its new and unique electronic and optical properties. Graphene-based materials have great potential for practical applications in nanoelectronics [1, 2], energy storage [3], liquid crystal devices and transparent conductive film, nanoelectro-mechanical devices[4], polymer composites and biomedicine. Recently Few-layers graphene oxide (FGO) has emerged as a new material based on carbon at the nanoscale. Structurally, FGO is

similar to graphene, with a base of groups containing oxygen [5]. As these groups have a strong affinity for water molecules, graphene oxide is hydrophilic and can be easily dissolved in water and other solvents.

Porphyrin nanorods (PN) are aromatic macrocycles with a cyclic-tetrapyrrole structure, electron rich, characterized by a remarkably high extinction coefficient in the visible range. These nanorods are functional with a variety of chemical, biological and unique photophysical properties [6]. In addition, they absorb strongly on graphite surfaces. Porphyrin nanorods are of potential interest as they can play a major role in achieving a rapid transfer of energy with a minimum of loss [7, 8]. Given the advantages of non-covalent functionalization, which can avoid destruction of π-conjugated skeleton and loss of electronic properties of FGO, the process used in this work allows functionalization of FGO with PN obtained by self-assembly.

The FGO/PN prepared were characterized by SEM, steady-state photoluminescence, resonant Raman scattering, infrared, and X-ray diffraction techniques in order to probe the interfacial bonding and electronic interaction between FGO and PN. These interactions showed a strong effect on these nanocomposite transient photoluminescence properties, as has been shown in our previous work.

2. Experimental Set-up

Graphene oxide (GO) was synthesized by our modified Hummer's method [9, 10]. The well-dispersed GO sheets were prepared using (KMnO4/H2SO4), and then the precipitate was washed many times with de-ionized water. The final solution was diluted and sonicated for a major exfoliation of the oxidized sheets. PN were synthesized via an ionic self-assembly technique by mixing aqueous solutions of two porphyrin precursors using the same procedures developed by Wang and al. [11, 12]. Meso-tetrakis (4-phenylsulphonicacid) porphyrin ($H_2TPPS_4^{2-}$) dihydrochloride and Sn(IV) tetrakis(4-pyridyl)porphyrin ($SnTPyP^{2+}$) dichloride were purchased from Frontier Scientific and used without further purification. To obtain porphyrin self-assembly nanorods, equal volumes of an acidified $H_2TPPS_4^{2-}$ solution (10.5 μM) and a Sn (IV)-tetrakis (4-pyridyl) porphyrin ($Sn(IV)TPyP^{2+}$) dichloride solution (3.5 μM) were mixed and left undisturbed in the dark for ~72 hours at room temperature. Rod formation is very sensitive to solution conditions, especially pH, because it alters the charge balance; hence, the synthesis was conducted under acidic conditions of pH ~2. First, the solution of the porphyrin nanorods was mixed with FGO, and then the obtained mixture was put into an ultrasound bath for 15 min at room temperature to insure homogeneity. Finally, a thin film of the FGO-PN composite was deposited by drop casting on a glass slide, which was rinsed with distilled water and acetone, and dried in an oven.

SEM images were obtained using a JEOL JSM 7600F and steady-state photoluminescence measurements were carried out at room temperature with a Jobin Yvon Fluorolog-3 spectrometer using a Xenon lamp (500 W) and a CCD detector. Raman spectra were carried out using a Bruker spectrometer SENTERRA Raman Stokes and a spectral range of 90-3200 cm^{-1} with an excitation wavelength λ = 785 nm; for our samples the laser power was adjusted to a low power 10 mW. A Jobin Yvon T64000 Raman spectrometer was used to record spectra at excitation wavelength of 514 nm; laser power was adjusted to 7 mW. Infrared absorption measurements were performed using a Fourier transform VERTEX 70 Series FT-IR spectrometer. X-ray diffraction (XRD) patterns of FGO, porphyrin nanorods and composites were established with Bruker's D8 advanced X-ray diffractometer using CuKα radiation (λ=1.5418 Å).

3. Results and Discussion

3.1 SEM

Scanning electron microscopy (SEM) images show graphene oxide layers and FGO-PN. The FGO images (Fig. 1(a)) present a network of randomly oriented sheet-like structures, and a wrinkled texture was observed. The SEM images of the FGO-porphyrin nanorods composite materials reveal that a better exfoliation of FGO and a good degree of homogeneity with a micrometre order of magnitude were achieved, resulting in the uniform and dense surface observed in Fig. 1(b). TEM images of PN aggregates and their disaggregation after their interaction with FGO can be seen in our previous work [13].

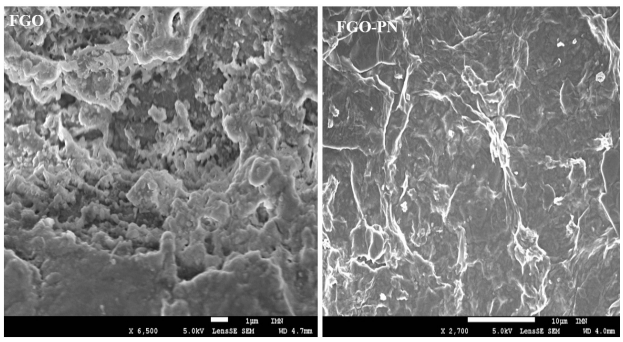

Figure 1. SEM images of FGO and FGO-PN

3.2 Steady-state Photoluminescence

Steady-state photoluminescence is widely used to investigate the efficiency of charge carrier trapping, migration and charge transfer and to understand the behaviour of electron-hole pairs in nanoparticles. Fig. 2 shows the PL spectra acquired at room temperature and under excitation wavelength of 420 nm for FGO, PN and FGO/PN composite. The PL spectrum of GO shows similar peaks to the results reported in the literature for as-produced GO [14, 15]. These peaks originate from the recombination of electron-hole (e-h) pairs, localized within small sp^2 carbon clusters embedded within a sp^3 matrix and agglomeration phenomena. Recently, Thomas et al. [15] have shown that as-produced GO con-

tains a mixture of lightly oxidized graphene-like sheets, together with heavily oxidized low-molecular-weight materials. These authors suggest that the intense PL observed for GO is due to the presence of oxidative debris on the surface of the graphene-like sheets. The presence of this oxidative debris will play an important role in the interaction of FGO with nanostructured PN. The steady-state photoluminescence spectrum of PN exhibits bands of around 640 and 714 nm, associated with 0–0 and 0–1 transitions [16]; these peaks are characteristics of porphyrin monomers and J-aggregated, respectively [13, 17].

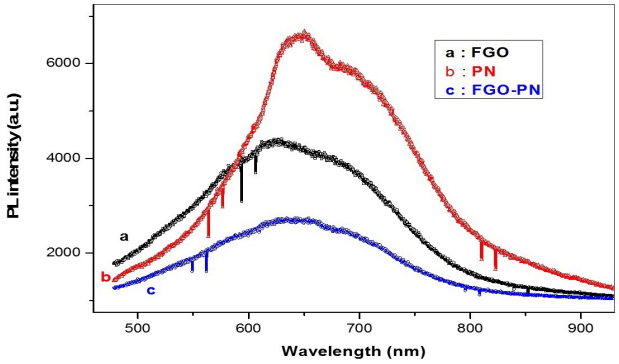

Figure 2. Steady-state photoluminescence acquired at 420 nm for FGO (a), FGO-PN (c) and PN (b)

It is to be noted that the PL intensity of the PN spectrum drops when the FGO is inserted in the PN solution, indicating the high probability of electron-hole recombination in PN [18]. The emission intensity was significantly weakened by introduction of FGO [19]. It is known that the PL emission is the result of recombination of excited electron-hole pairs; lower PL intensity indicates a lower electron-hole recombination rate. Thus, FGO plays an important role in accepting the electrons photogenerated, a necessary factor to improve the photocatalytic activity of PN-FGO [20].

The PL quenching and the band shift of PN/FGO composite excited at 420 nm, in resonance with the Soret band of the PN, is due to charge/energy transfer between the PN and GO sheets. The decrease of the PL intensity of the FGO indicates that the mixture of PN solution at pH = 2 with FGO solution can lead to a quenching of the FGO PL. This behaviour may originate from the debris contained in FGO, as reported in previous work by Thomas et al. [15], which interacts with the PN leading to a quenching of the FGO PL. Our results show that one can modulate the PL of this nanocomposite by controlling the pH and concentration of the nanostructured PN.

3.3 Resonant Raman Scattering

Resonant Raman spectra of the FGO and porphyrin nanorods obtained at different excitation wavelengths 514 and 785 nm are shown in Figs. 3(a) and (b). These excitation wavelengths are in resonance with PN aggregate absorption bands presented in our previous work [13]. The fluorescence was automatically subtracted by the spectrometer. In Fig. 3(a), with 514 nm excitation, the Raman spectra exhibit two prominent peaks, of the D band and G band, as well as a weak and broad 2D band, which is typical of chemically derived graphene; it can also be used to determine the number of sheets in GO. Fig. 3(b), 785 nm excitation, shows Raman spectra of FGO, PN and composites. The FGO spectrum displays a D band located at 1306 cm^{-1}, characteristic of defects present on its surface; a G-band is observed around 1595 cm^{-1} and corresponds to the E2g mode [21, 22]. In the case of the PN, which show resonance behaviour, the 514 nm excitation enhances vibrational bands at low frequencies. The band centred at 1236 cm^{-1} can be attributed to the stretching of the C_m-C_ϕ bond; the band at 1386 cm^{-1} is related to the asymmetrical stretching of the C_α-C_β-NH bonds [23, 24]; the band at 1526 cm^{-1} originates from the stretching of the C_β-$C_{\beta'}$ bond; and the band centred at 1637 cm^{-1} corresponds to the C-C stretching bond in the phenyl ring [25]. The spectrum of the composite FGO-PN shows the two main bands of FGO overlapping with the PN bands; the D band at 1318 cm^{-1} and the G-band at around 1600 cm^{-1} may be attributed to the carbon-carbon stretching. Generally, the ratio of the intensities (I_D/I_G) of the two bands D and G is used to provide additional information on the quality of the nanostructured carbon-based materials. It is well known that the quality decreases when the I_D/I_G ratio increases [26, 27].

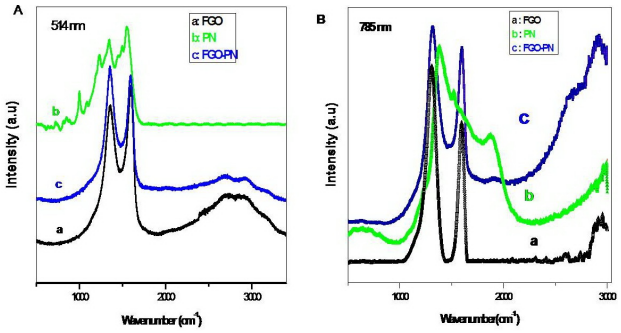

Figure 3. Resonant Raman spectra recorded at 514 nm and 785 nm for FGO (a), PN (b) and composite FGO-PN (c)

It can be seen that the intensity ratio of FGO-PN (I_D/I_G = 1.44) increases with respect to the GO ratio (I_D/I_G = 1.40), which is consistent with the introduction of defects on the FGO surface. These changes may be due to the π-π interaction between the FGO and PN, which is in agreement with results presented recently by other researchers [28].

3.4 FT-IR Measurements

In the graphene oxide (FGO) FT-IR spectrum (Fig. 4) we observe the bands located at 1226 cm^{-1} and 1420 cm^{-1}, and 1620 cm^{-1} may be respectively attributed to C-OH and C=C stretching. The peak at 1718 cm^{-1} may be assigned to C=O stretching of the carboxylic group [27, 29]. In relation to the

porphyrin nanorods we note the presence of a broad intense band centred at 3400 cm^{-1}, which is attributed to N-H stretching, and the band situated at 2914 cm^{-1} is related to the stretching vibration of aromatic C-H bonds. In addition, a band is observed at around 1629 cm^{-1} and corresponds to the C=C stretching in the phenyl nuclei. Moreover, the band at 1540 cm^{-1} is attributed to C_{β}-$C_{\beta'}$ stretching, which may be due to symmetrical deformation of the pyrrole rings and the bending strain C_{α}-N-$C_{\alpha'}$. The band at 1415 cm^{-1} is attributed to the symmetric stretching of C_{α}-N-$C_{\alpha'}$ and the C_{β}-$C_{\beta'}$ bond stretching in pyrrole nuclei; there is also a band which appears at 1318 cm^{-1} corresponding to the asymmetric HN-C_{α}-C_{β} stretching bond. The peak at 1261 cm^{-1} may be assigned to the asymmetric C_{α}-N-$C_{\alpha'}$ stretching [23, 30]. In FGO-PN we find that the relative intensities of these bands change significantly. Moreover, the absence of the band at 1408 cm^{-1} and the shift of the N-H band indicate a strong interaction between FGO and PN [28], confirming our results obtained by resonant Raman spectroscopy and steady-state photoluminescence.

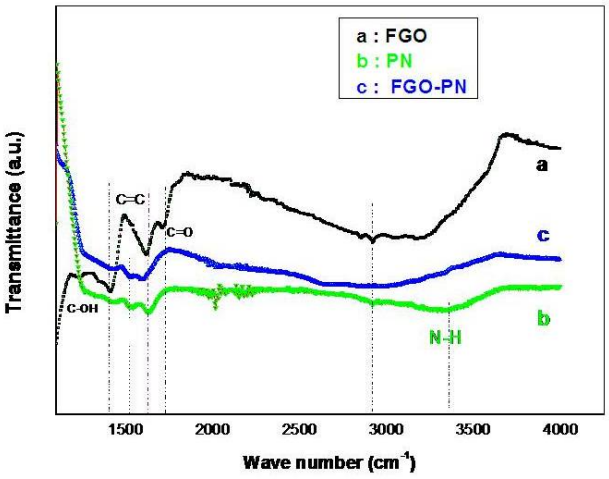

Figure 4. FT-IR spectra of FGO (a), PN (b) and composite FGO-PN (c)

3.5 X-Ray Diffraction

Dummy Text Fig. 5 shows the XRD patterns of FGO, PN, and FGO-PN. The FGO spectrum exhibits an intense and strong peak at 2θ = 11.4°, which is attributed to the (001) lattice spacing of 0.78 nm due to the interlamellar water trapped between the hydrophilic graphene-oxide layers [29, 31, 32]. For porphyrin nanorods the XRD patterns show a strong peak at 2θ =31.75°, attributed to the (701) [33, 34]. The FGO-PN composite shows a peak at 2θ = 10.03° (d-spacing = 0.881 nm); this can be explained by the increase of the inter-planar distance (001) due to the effect of PN trapped by FGO. The increase in the intensity ratio (I_D/I_G) observed in Raman spectra corresponding to the FGO surface modification after the intercalation of PN and XRD results is in agreement with this observation.

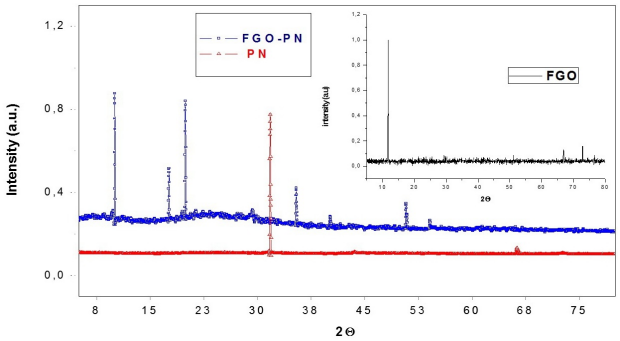

Figure 5. XRD patterns of FGO, PN and FGO-PN

4. Conclusion

The morphological, structural and optical properties of PN and their interactions with FGO have been investigated. SEM showed good adhesion and exfoliation of FGO in PN. The interaction with FGO was seen to alter the aggregate structure of the PN. Strong π-π interaction and charge/energy transfer between PN and FGO were confirmed by photoluminescence, resonant Raman spectroscopy and FT-IR, suggesting that FGO functionalized with nanostructure PN, with their tuneable structural and optical properties, can yield new opportunities for optic limiting, optoelectronics and photovoltaic devices.

5. References

[1] Li X, Wang X, Zhang L, Lee S, Dai H (2008) Chemically Derived Ultrasmooth Graphene Nanoribbon Semiconductors. Science 319: 1229-1232.

[2] Kamat P V (2011) Graphene-Based Nanoassemblies for Energy Conversion. J. Phys. Chem. Lett. 2 (3): 242-251.

[3] Stoller M D, Park S, Stoller, Zhu Y, An J, and Ruoff R S (2008) Graphene-Based Ultracapacitors. Nano Lett. 8: 3498-3502.

[4] Kim B -Ja, Mastro M A, Hite J, Eddy Jr C R and Kim J (2010) Transparent conductive graphene electrode in GaN-based ultra-violet light emitting diodes. Optics Express 18: 23030-23034.

[5] Dreyer D R, Park S, Bielawski C W and Ruof R S (2010) The chemistry of graphene oxide. Chem.Soc.Rev. 39: 228-240.

[6] Lindgren B M A M (2009) Vibration and Fluorescence Spectra of Porphyrin-Cored 2, 2-Bis(methylol)-propionic Acid Dendrimers. Sensors 9: 1937-1966.

[7] Franco R, Jacobsen J L, Wang H, Wang Z, Istva'n K, Schore N E, Song Y, Medforthcd C J and Shelnutt J A (2010) Molecular organization in self-assembled binary porphyrin nanotubes revealed by resonance Raman spectroscopy. Phys. Chem. Chem. Phys. 12: 4072-4077.

[8] Kiessling D, Katsukis G, Malig J, Lodermeyer F, Feihl S, Roth A, Wibmer L, Kehrer M, Volland M, Wagner P, Wallace G G, Officer D L and Guldi D M (2013) Novel nanographene/porphyrin hybrids-preparation, characterization, and application in solar energy conversion schemes. Chem. Sci. 4: 3085-3098.

[9] Dreyer D R, Park S, Bielawski C W and Ruof R S (2010) The chemistry of graphene oxide. Chemical Society Reviews 39: 228-240.

[10] Khenfouch M, Baitoul M, Maaza M (2014) Raman study of graphene/nanostructured oxides for optoelectronic applications. Optical Materials 36: 27-30.

[11] Mongwaketsi N, Ndungu P G, Nechaev A, Maaza M, and Sparrow R (2010) Ionic self-assembly of porphyrin nanostructures on the surface of charge-altered track-etched membranes. Journal of Porphyrins and Phthalocyanines 14: 446-451.

[12] Mongwaketsi N, Khamlich S, Klumperman B, Sparrow R, Maaza M (2012) Synthesis and characterization of porphyrin nanotubes/rods for solar radiation harvesting and solar cells. Physica B 407: 1615-1619.

[13] Khenfouch M, Baïtoul M, Maaza M, Wéry J (2014) Photoluminescence and dynamics of excitation relaxation in graphene oxide-porphyrin nanorods composite. Journal of Luminescence 145: 33-37.

[14] Chien C -Ta, Li S -S, Lai W -J, Yeh Y -C, Chen H -A, Chen I -S, Chen L - C, Chen K -H, Nemoto T, Isoda S, Chen M, Fujita T, Eda G, Yamaguchi H, Chhowalla M, and Chen C -W (2012) Tunable Photoluminescence from Graphene Oxide. Angew. Chem. Int. 51: 6662-6666.

[15] Thomas H R, Valles C, Young R J, Kinloch I A, Wilson N R and Rourke J P (2013) Identifying the fluorescence of graphene oxide. J. Mater. Chem. C 1: 338-342.

[16] Bala Murali Krishna M, Venkatramaiah N, Venkatesanb R and Narayana Rao D (2012) Synthesis and structural, spectroscopic and nonlinear optical measurements of graphene oxide and its composites with metal and metal free porphyrins. J. Mater. Chem. 22: 3059-3068.

[17] Serpone N (1999) Photoluminescence and Transient Spectroscopy of Free Base Porphyrin Aggregates. J. Phys. Chem. B 1, 103: 761-769.

[18] Wiglusz R, Legendziewicz J, Radzki S, Gawryszewskaa P, Sokolnicki J (2004) Spectroscopic properties of porphyrins and effect of lanthanide ions on their luminescence efficiency. Journal of Alloys and Compounds 380: 396-404.

[19] Loh K P, Bao Q, Eda G and Chhowalla M (2010) Graphene oxide as a chemically tunable platform for optical applications. Naturechemistry 2: 1015-1024.

[20] Liu Z D, Zhao H X, Huang C Z (2012) Obstruction of Photoinduced Electron Transfer from Excited Porphyrin to Graphene Oxide: A Fluorescence Turn-On Sensing Platform for Iron (III) Ions. PLOS ONE 7: 1-8.

[21] Shen J, Li N, Shi M, Hu Y, Ye M (2010) Covalent synthesis of organophilic chemically functionalized graphene sheets. Journal of Colloid and Interface Science 348: 377-383.

[22] Ferrari A C (2007) Raman spectroscopy of graphene and graphite: Disorder, electron-phonon coupling, doping and nonadiabatic effects. Solid State Communications 143: 47-57.

[23] Aydin M (2013) DFT and Raman spectroscopy of porphyrin derivatives: Tetraphenylporphine (TPP). Vibrational Spectroscopy 68: 141-152.

[24] Wan J, Wang H, Wu Z, Shun Y C, Zheng X and Phillips D L (2011) Resonance Raman spectroscopy and density functional theory calculation study of photodecay dynamics of tetra(4-carboxyphenyl) porphyrin. Phys. Chem. Chem. Phys 13: 10183-10190.

[25] Elliott A B S, Gordon K C, Khoury T, Crossley M J (2012) Probing the electronic structure of b; b0-fused quinoxalino porphyrins and tetraazaanthracene-bridged bis-porphyrins with resonance Raman spectroscopy and density functional theory. Journal of Molecular Structure 1029: 187-198.

[26] Ferrari A C, Robertson J (2001) Resonant Raman spectroscopy of disordered, amorphous, and diamondlike carbon. Physical Review B 64: 1-13.

[27] Sutar P K N D S, Singh G, Divakar Botcha V, Talwar S S, Srinivasa R S, Major S S (2012) Spectroscopic studies of large sheets of graphene oxide and reduced graphene oxide monolayers prepared by Langmuir-Blodgett technique. Thin Solid Films 520: 5991-5996.

[28] Zhu M, Li Z, Xiao B, Lu Y, Du Y, Yang P, and Wang X (2013) Surfactant Assistance in Improvement of Photocatalytic Hydrogen Production with the Porphyrin Noncovalently Functionalized Graphene Nanocomposite. ACS Appl. Mater. 5: 1732-1740.

[29] Bykkam S, Venkateswara R K, Shilpa Chakra C H and Thunugunta T (2013) Synthesis and characterization of graphene oxide and its antimicrobial activity against Klebseilla and Staphylococus. International Journal of Advanced Biotechnology and Research 4: 142-146.

[30] Alben J, Choi S S (1973) Infrared apectroscopy of porphyrins. Annals New York Academy of Sciences 206: 278-294.

[31] Khenfouch M, Baitoul M, Maaza M (2012) White photoluminescence from a grown ZnO nanorods/

graphene hybrid nanostructure. Optical Materials 34: 1320-1326.

[32] Pham V H, Dang T T, Hur S H, Kim E J, Kong B S, Kim S and Chung J S (2012) Chemical reduction of an aqueous suspension of graphene oxide by nascent hydrogen. J. Mater. Chem. 22: 10530-10536.

[33] Hu J -S, Liang H -P, Wan L -J, and Jiang L (2005) Three-Dimensional Self-Organization of Supramolecular Self-Assembled Porphyrin Hollow Hexagonal Nanoprisms. J. Am. Chem. Soc. 127: 17090-17095.

[34] Wang L, Chen L Y, Jiang J (2014) Controlling the growth of porphyrin based nanostructures for tuning third-order NLO properties. Nanoscale 6: 1871-1878.